

Andreev reflection and cyclotron motion at superconductor – normal-metal interfaces

F. Giazotto,¹ M. Governale,¹ U. Zülicke,² and F. Beltram¹

¹*NEST-INFM and Scuola Normale Superiore, Piazza dei Cavalieri 7, I-56126 Pisa, Italy*

²*Institute of Fundamental Sciences and MacDiarmid Institute for Advanced Materials and Nanotechnology, Massey University, Private Bag 11 222, Palmerston North, New Zealand*

(Dated: April 8, 2018)

We investigate Andreev reflection at the interface between a superconductor and a two-dimensional electron system (2DES) in an external magnetic field such that cyclotron motion is important in the latter. A finite Zeeman splitting in the 2DES and the presence of diamagnetic screening currents in the superconductor are incorporated into a microscopic theory of Andreev edge states, which is based on the Bogoliubov–de Gennes formalism. The Andreev–reflection contribution to the interface conductance is calculated. The effect of Zeeman splitting is most visible as a double–step feature in the conductance through clean interfaces. Due to a screening current, conductance steps are shifted to larger filling factors and the formation of Andreev edge states is suppressed below a critical filling factor.

PACS numbers: 74.45.+c, 71.70.Di, 73.20.-r, 73.40.-c

I. INTRODUCTION

The trend toward radical miniaturization of electronic devices has spurred efforts aimed at understanding the effect of quantum coherence on transport. Current research is investigating a variety of such *mesoscopic* systems.^{1,2,3} Recently, the subject of *mesoscopic superconductivity*^{4,5,6} has attracted considerable interest, partly due to the possibility to perform experiments in hybrid structures consisting of superconductors and semiconductors where phase-coherence lengths exceed device dimensions.⁷ Many effects observed in these systems ultimately stem from *Andreev reflection*.^{8,9} Speaking in simple terms, Andreev reflection occurs at the interface between a superconductor (S) and a normal metal (N) when an electron with energy within the superconducting gap is incident on the interface from the N side. While no states are available in S for the incoming electron, a finite amplitude for pairing with some suitable electron from N is induced by the proximity of S, which allows both electrons to enter S as a Cooper pair. If that happens, N is left with a hole excitation that has the sign of its group velocity, charge, and mass opposite to that of the electron. As incoming electron and Andreev-reflected hole have a definite phase relation, bound states are formed in multi-interface geometries such as S–N–S¹⁰ or S–N–I¹¹ systems, giving rise to discrete energy levels within the superconducting gap.

An external magnetic field $\vec{B} = \vec{\nabla} \times \vec{A}$ affects transport properties of mesoscopic systems at least in two ways. In systems with finite Zeeman splitting (given by $g\mu_B B$, g being the gyromagnetic factor and μ_B the Bohr magneton), spin degeneracy is lifted, which turns out to suppress Andreev reflection.^{12,13,14} In addition, the vector potential \vec{A} explicitly enters the single–electron Hamiltonian,

$$H_0 = \frac{1}{2m} (\vec{p} - e\vec{A})^2 + \frac{g}{2} \mu_B \vec{\sigma} \cdot \vec{B} \quad , \quad (1)$$

resulting in a host of peculiar quantum-mechanical effects. One of the most well-known is perhaps the appearance of phase factors which lead to magnetoconductance oscillations in a variety of mesoscopic systems³ and affect orbital wave

functions even in regions where no magnetic field is present.¹⁵ If the magnetic field is treated within a quasiclassical approximation which assumes the relevant physical length scale of the system to be much smaller than the cyclotron radius of electrons, the Hamiltonian of Eq. (1) reduces to

$$H_0^{(qc)} = \epsilon_F + v_F \hat{p} \cdot (\vec{p} - e\vec{A}) + \frac{g}{2} \mu_B \vec{\sigma} \cdot \vec{B} \quad , \quad (2)$$

and modifications of orbital wave functions due to the magnetic field arise entirely from such phase factors. Here, $\epsilon_F = \hbar^2 k_F^2 / (2m)$, $v_F = \hbar k_F / m$, and k_F are the Fermi energy, Fermi velocity, and Fermi wavevector, respectively. Most of the previous studies of Andreev reflection in a magnetic field were carried out in the quasiclassical limit.^{11,16,17,18,19,20,21,22,23}

The quasiclassical approximation ceases to be valid, however, when the cyclotron radius $r_c = l_B^2 k_F$ is smaller than the characteristic length scales of the system which are set, e.g., by disorder, temperature, or size (here, $l_B = (\hbar / |e\vec{B}|)^{1/2}$ denotes the *magnetic length* which is the fundamental quantum-mechanical length scale introduced by the magnetic field.) In this limit, another well-known quantum effect due to the magnetic field becomes important, which is Landau quantization²⁴ of electron motion in planes perpendicular to the field direction. In transport, Landau quantization manifests itself, e.g., by Shubnikov – de Haas oscillations and by the quantum Hall effect.^{25,26} Recent advances in fabrication technology make it possible to study Andreev reflection in superconductor–semiconductor hybrid systems at magnetic fields where cyclotron motion of quasiparticles can be important in the semiconducting region,^{27,28,29,30,31} motivating a number of related theoretical studies.^{32,33,34,35,36,37,38,39,40}

Here we present results on the interplay between Andreev reflection and cyclotron motion at S–N interfaces. We focus in particular on the effect of a finite Zeeman splitting in the normal region and on the impact of the diamagnetic screening current in the superconductor.⁴¹ To be specific, we choose a geometry where $\vec{B} = B \hat{z}$ and the interface is the yz plane. Considering particle motion in the xy plane from a classical point of view, the interplay between cyclotron motion and Andreev reflection at an ideal interface results in electrons and

holes alternating in skipping orbits along the interface^{42,43} in y direction, as shown in Fig. 1. In quantum mechanics, however, the guiding-center coordinates for cyclotron orbits are canonically conjugate operators which cannot be diagonalized simultaneously⁴⁴ while each of them separately commutes with H_0 . In the present problem, where translational invariance is broken due to the interface, it is useful to choose the representation where the guiding-center coordinate X in x direction is a good quantum number, i.e., eigenstates of H_0 are labeled by X . Details of our quantum-mechanical description of the S–N interface in a magnetic field are given in the following section. It is based on finding solutions of the Bogoliubov – de Gennes (BdG) equation,⁴⁵

$$\begin{pmatrix} H_0 + U - \epsilon_F & |\Delta| e^{2i\varphi} \\ |\Delta| e^{-2i\varphi} & -H_0^* - U + \epsilon_F \end{pmatrix} \begin{pmatrix} u \\ v \end{pmatrix} = E \begin{pmatrix} u \\ v \end{pmatrix}, \quad (3)$$

for the hybrid system by matching at the interface appropriate solutions for the S and N regions.⁴⁶ Scattering at the interface is modeled by an external potential $U = U(x) = U_0 \delta(x)$. We allow for different effective masses and Fermi energies in the S and N regions. For our study, we adopt the model where the relevant quasiparticle excitations in the S region are those of a conventional BCS s-wave superconductor with a uniform superflow in the y direction parallel to the interface due to the presence of diamagnetic screening currents. This approach is strictly valid only when S is a type-II superconductor in the Meissner or diluted–vortex phases. To be specific, we consider exactly this case in Sec. II, but discuss generalizations to the mixed phase in the Discussion section. The motion in z direction, i.e., parallel to the magnetic field, can be trivially separated and gives only rise to an additive renormalization of the Fermi energy. We shall neglect this in the following, making our study especially applicable for S–N junctions where the N region is a two–dimensional electron system. Eigenenergies for the motion in the xy plane in a uniform magnetic field are labelled by the guiding-center quantum number X and correspond to the familiar Landau levels of independent electrons and holes when $|X| \gg r_c$. Similar to the case of a hard wall,^{47,48} Landau levels are bent for X close to the S–

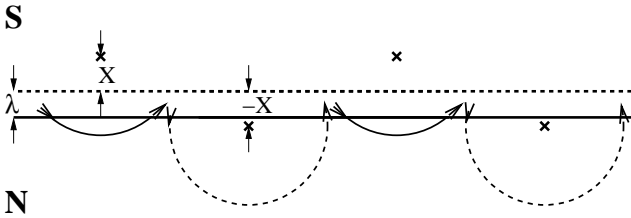


FIG. 1: Semiclassical picture of Andreev edge states. Electrons and holes in skipping orbits along a clean S–N interface are successively Andreev–reflected into each other. In the S region, quasiparticle excitations exist only on the (extremely short) length scale of the superconducting coherence length. The presence of a uniform supercurrent parallel to the interface results in a shift of electron and hole orbits in the normal region. Andreev reflection couples electron and hole orbits with guiding-center coordinate $\pm X - \lambda$, respectively. λ denotes the magnetic penetration depth.

N interface, and the corresponding eigenspinors of the BdG equation are of mixed electron-hole type. An example of the spectrum of such solutions with energies within the superconducting gap was given in Ref. 33.

The classical picture of skipping orbits along the interface, and the analogy with the familiar quantum-Hall edge states,^{47,48,49,50} suggests that currents will flow along the interface in the plane perpendicular to \vec{B} (i.e., in y direction). In superconductivity, *quasiparticle* current $\vec{j}_P = \vec{j}_e + \vec{j}_h$ and *charge* current $\vec{j}_Q = e(\vec{j}_e - \vec{j}_h)$ are distinguished where, for a particular solution of the BdG equation, electron and hole currents are given by⁴⁵

$$\vec{j}_e = \frac{1}{m} \Re \left\{ u^* \left(\vec{p} - e\vec{A} \right) u \right\}, \quad (4a)$$

$$\vec{j}_h = \frac{1}{m} \Re \left\{ v \left(\vec{p} - e\vec{A} \right) v^* \right\}. \quad (4b)$$

It turns out³³ that \vec{j}_e and \vec{j}_h are always parallel to the interface for states with definite guiding-center coordinate X in the direction perpendicular to the interface. This is no surprise because, owing to the peculiar quantum dynamics in a magnetic field, the guiding center for electrons and holes cannot be localized in y direction in a state where it is fixed in the x direction. Generalizing the Hellmann-Feynman theorem⁵¹ to the matrix BdG Hamiltonian of Eq. (3), a general expression can be derived³³ for the contribution of a particular eigenstate (u_{nX}, v_{nX}) with energy E_{nX} , labelled by Landau-level index n and guiding-center quantum number X , to the *total* quasiparticle and charge currents in y direction:

$$I_{nX}^{(P,Q)} = \int_x (\vec{j}_{P,Q})_y. \quad (5)$$

The total quasiparticle current turns out not to depend explicitly on the electron or hole wavefunctions. Rather, it is given entirely in terms of the energy spectrum,

$$I_{nX}^{(P)} = \frac{1}{\hbar} \frac{\ell^2}{L_y} \frac{\partial E_{nX}}{\partial X}, \quad (6)$$

which acquires a nonzero dispersion only close to the S–N interface. Hence, confinement due to the interface with a superconductor gives rise to the formation of a chiral *edge channel for quasiparticle current* in exactly the same way as confinement due to a hard wall induces edge channels for charge current.^{47,48} We distinguish the new kind of edge channel realized at the S–N interface from its counterpart near a hard wall by calling it an *Andreev edge channel* and call the solutions (u_{nX}, v_{nX}) of the BdG equation with nonzero $I_{nX}^{(P)}$ *Andreev edge states*. [In Eq. (6), L_y denotes the system size in y direction.] As expected intuitively, the total charge current $I_{nX}^{(Q)}$ flowing in an Andreev edge state *does* depend on the details of the wave functions; it can be written as $I_{nX}^{(Q)} = I_{nX}^{(H)} + I_{nX}^{(S)}$. The expression for $I_{nX}^{(H)}$ suggests a straightforward interpretation.³³ It is given by

$$I_{nX}^{(H)} = \frac{e}{\hbar} \frac{\ell^2}{L_y} \frac{\partial E_{nX}}{\partial X} (1 - 2 B_{nX}), \quad (7)$$

where $B_{nX} = \int_x |v_{nX}|^2$ is the hole probability in the Andreev edge state. Equation (7) is the expression for current in an edge channel that is *reduced* due to the presence of Andreev reflection. For vanishing B_{nX} , i.e., when only normal reflection occurs at the S–N interface, Andreev edge channels actually become the familiar quantum-Hall edge channels.^{47,48,49,50} Inspection shows that the term $I_{nX}^{(S)}$ represents the quasiparticle–conversion current in the superconductor that supports the Andreev edge state. Note that the above discussion, as well as the analytic expressions, for currents are generally valid, i.e., in particular also with finite Zeeman splitting and diamagnetic screening currents present. It is then possible³³ to express the Andreev–reflection contribution to the S–N interface conductance in terms of the hole probabilities of zero–energy Andreev edge states as

$$G_{\text{AR}} = \frac{e^2}{\pi\hbar} \sum_n' B_n, \quad (8)$$

where the label n comprises the set of quantum numbers (Landau–level index and spin–projection eigenvalue) for zero–energy eigenstates, and the \sum_n' indicates that only electron-like states (i.e., those with $B_n < 1/2$) are to be summed over. As the experimentally relevant quantity, we present results for G_{AR} in the following.

We continue with presenting our model of an S–N junction subject to a quantizing magnetic field in Sec. II. (Readers not interested in the mathematical formalism can skip this section.) Numerical results obtained within that model are reported in Sec. III, where the effects of Zeeman splitting and diamagnetic supercurrents are elucidated in detail. We discuss implications of these results with particular emphasis on experimentally realizable superconductor–semiconductor hybrid structures. Conclusions are given in the final Sec. IV.

II. MODEL OF AN S–N HYBRID SYSTEM IN A QUANTIZING MAGNETIC FIELD

Our model of the S–N interface is similar, in spirit, to that used in the approach by Blonder, Tinkham, and Klapwijk⁴⁶ (BTK) and its recent generalizations to superconductor–semiconductor interfaces.⁵² We consider a planar hybrid system (in the xy plane) consisting of a semi-infinite two-dimensional electron system (2DES, located in the half-plane $x > 0$) and a superconductor (occupying the half-plane $x < 0$). The effective mass of electrons, the Fermi energy, and the modulus of the superconducting pair potential are assumed to be piecewise constant as functions of the coordinate perpendicular to the interface:

$$m(x) = m_s \Theta(-x) + m_n \Theta(x) \quad , \quad (9a)$$

$$\epsilon_F(x) = \epsilon_{F,s} \Theta(-x) + \epsilon_{F,n} \Theta(x) \quad , \quad (9b)$$

$$|\Delta|(x) = \Delta_0 \Theta(-x) \quad . \quad (9c)$$

The magnetic field, applied perpendicular to the 2DES, is assumed to be screened from the S region,

$$\vec{B}(x) = \{B e^{\frac{x}{\lambda}} \Theta(-x) + B \Theta(x)\} \hat{z} \quad , \quad (10a)$$

where λ denotes the magnetic penetration depth. Translational invariance in y direction suggests a gauge for the vector potential where $\vec{A} = A(x) \hat{y}$, and we choose

$$A(x) = \lambda B (e^{\frac{x}{\lambda}} - 1) \Theta(-x) + x B \Theta(x) \quad . \quad (10b)$$

In the presence of a magnetic field, the phase 2φ of the superconducting pair potential acquires a non-trivial dependence on spatial coordinates, and care has to be taken to determine it correctly.^{16,19} Combining Maxwell and London equations,

$$\vec{\nabla} \times \vec{B} = \mu_0 \vec{j}_s \quad , \quad (11a)$$

$$\vec{j}_s = \frac{\hbar}{e\mu_0\lambda^2} \vec{k}_s \quad , \quad (11b)$$

where \vec{j}_s is the screening supercurrent, and

$$\vec{k}_s = \vec{\nabla}\varphi - e\vec{A} \quad , \quad (12)$$

we obtain from Eqs. (10) for the case under consideration

$$\varphi(y) = -\frac{\lambda}{l_B^2} y \operatorname{sgn}(eB) + \varphi_0 \quad , \quad (13)$$

with $\operatorname{sgn}(x)$ denoting the sign function, and φ_0 a constant.

We calculate electronic and transport properties from solutions of the BdG equation (3). Upon making the separation *Ansätze*

$$u(x, y) = \frac{1}{\sqrt{L_y}} f_X(x) e^{i[\varphi(y)+y\frac{x}{l_B^2} \operatorname{sgn}(eB)]} \quad , \quad (14a)$$

$$v(x, y) = \frac{1}{\sqrt{L_y}} g_X(x) e^{i[-\varphi(y)+y\frac{x}{l_B^2} \operatorname{sgn}(eB)]} \quad , \quad (14b)$$

and using the fact that, in the presence of Zeeman splitting, Eq. (3) exhibits a block–diagonal form⁵³ in the spin quantum number σ , we find a onedimensional BdG equation,

$$\begin{pmatrix} H_{+, \sigma} + U & |\Delta| \\ |\Delta| & -H_{-, -\sigma} - U \end{pmatrix} \begin{pmatrix} f_{X, \sigma} \\ g_{X, -\sigma} \end{pmatrix} = E \begin{pmatrix} f_{X, \sigma} \\ g_{X, -\sigma} \end{pmatrix} . \quad (15)$$

The single-particle Hamiltonians $H_{\pm, \sigma}$ are different in the S and N regions, $H_{\pm, \sigma} = \Theta(-x) H_{\pm, \sigma}^{(s)} + \Theta(x) H_{\pm, \sigma}^{(n)}$, where

$$H_{\pm, \sigma}^{(n)} = \frac{\hbar\omega_c}{2} \left\{ \frac{l_B^2}{\hbar^2} p_x^2 + \left[\frac{x + \lambda \mp X}{l_B} \right]^2 + \sigma\eta_Z - \nu \right\} . \quad (16)$$

Here $\omega_c = \hbar/(m_n l_B^2)$ denotes the cyclotron frequency in the N region, $\eta_Z = g\mu_B B/(\hbar\omega_c)$ measures Zeeman splitting, and $\nu = 2\epsilon_{F,n}/(\hbar\omega_c)$ is the filling factor. In the superconductor, the single-particle Hamiltonian depends on the superflow wave vector $\vec{k}_s = k_s \hat{y}$,

$$k_s = -\frac{\lambda}{l_B^2} e^{\frac{x}{\lambda}} \operatorname{sgn}(eB) \Theta(-x) \quad , \quad (17a)$$

$$H_{\pm, \sigma}^{(s)} = \frac{p_x^2}{2m_s} + \frac{\hbar^2 [X \pm l_B^2 k_s \operatorname{sgn}(eB)]^2}{2m_s l_B^4} - \epsilon_{F,s} \quad (17b)$$

Here we have neglected Zeeman splitting in the S region, which is a good approximation for typical field strengths applied experimentally in S–2DES hybrid structures. For our purposes, we need to find solutions of Eq. (15) in the S region on length scales $x \sim \xi_0$ where ξ_0 is the superconducting coherence length. In a type-II material which has $\xi_0 \ll \lambda$, we can approximate $\exp\{x/\lambda\} \approx 1$ in Eq. (17a) and use

$$H_{\pm, \sigma}^{(s)} \approx \frac{p_x^2}{2m_s} + \frac{\hbar^2}{2m_s l_B^4} (X \mp \lambda)^2 - \epsilon_{F, s} \quad (17c)$$

Our approximation amounts to neglecting the cyclotron motion of evanescent quasiparticles in the S region, which translates into the condition that the superconducting gap parameter Δ_0 is much larger than the cyclotron energy of electrons in the superconducting material. This is typically satisfied for realistic situations.

Solutions of Eq. (15) for the S–N system are found by matching *Ansätze* for eigenfunctions in the S and N regions at the interface $x = 0$. In the S region, where a uniform superflow with velocity $\hbar\lambda/(m_s l_B^2)$ is present, the appropriate *Ansatz* is a superposition of Doppler-shifted quasiparticle excitations,

$$\begin{pmatrix} f_{X, \sigma} \\ g_{X, -\sigma} \end{pmatrix}_{x < 0} = d_- \begin{pmatrix} \gamma_- \\ 1 \end{pmatrix} \psi_-(x) + d_+ \begin{pmatrix} \gamma_+ \\ 1 \end{pmatrix} \psi_+(x), \quad (18)$$

with functions $\psi_{\pm}(x) = \exp\{\mp i x q_{\pm}\}$, and parameters

$$q_{\pm} = \left[\frac{2m_s}{\hbar^2} \left(\epsilon_{F, s} \pm \sqrt{(E + \delta\lambda)^2 - \Delta_0^2} \right) - \frac{X^2 + \lambda^2}{l_B^4} \right]^{\frac{1}{2}} \quad (19a)$$

$$\gamma_{\pm} = \frac{\Delta_0}{E + \delta\lambda \mp \sqrt{(E + \delta\lambda)^2 - \Delta_0^2}}, \quad (19b)$$

$$\delta\lambda = \hbar\omega_c \frac{m_n}{m_s} \frac{X\lambda}{l_B^2}. \quad (19c)$$

For $|E + \delta\lambda| < \Delta_0$, the wave function displayed in Eq. (18) corresponds to evanescent quasiparticle excitations in S. The *Ansatz* for the wave function in the N region is a superposition of purely electron and hole-like BdG spinors,

$$\begin{pmatrix} f_{X, \sigma} \\ g_{X, -\sigma} \end{pmatrix}_{x > 0} = \begin{pmatrix} a \\ 0 \end{pmatrix} \chi_{+, \sigma}(\zeta_+) + \begin{pmatrix} 0 \\ b \end{pmatrix} \chi_{-, -\sigma}(\zeta_-), \quad (20)$$

where $\zeta_{\pm} = x + \lambda \mp X$, and the functions $\chi_{\pm, \sigma}(\zeta)$ are eigenfunctions of the harmonic-oscillator Schrödinger equation,

$$\frac{l_B^2}{2} \frac{d^2 \chi_{\pm, \sigma}}{d\zeta^2} - \left[\frac{\zeta^2}{2l_B^2} - \frac{\nu - \sigma\eta_Z}{2} \mp \frac{E}{\hbar\omega_c} \right] \chi_{\pm, \sigma} = 0, \quad (21)$$

normalized to unity in the half-space occupied by the N region. They can be expressed in terms of *parabolic cylinder functions*⁵⁴ that are well-behaved as $x \rightarrow \infty$,

$$\chi_{\pm, \sigma}(\zeta_{\pm}) = F_{\pm, \sigma} U \left(-\frac{\nu - \sigma\eta_Z}{2} \mp \frac{E}{\hbar\omega_c}, \sqrt{2} \frac{\zeta_{\pm}}{l_B} \right), \quad (22)$$

where $F_{\pm, \sigma}$ are normalization constants.

Imposing the continuity of BdG quasiparticle wave function and conservation of the probability current at the interface yields the secular equation

$$GH(c'^2 + d'^2) + G'H' = c' \frac{E + \delta\lambda}{\sqrt{\Delta_0^2 - (E + \delta\lambda)^2}} (G'H - GH') + d' (G'H + GH') \quad (23)$$

whose parameters are: $c' = \frac{m_n}{m_s} \Re\{q_+\}$, $d' = \frac{m_n}{m_s} \Im\{q_+\} + \tilde{U}$ with $\tilde{U} = \frac{2m_n}{\hbar^2} U_0$, $G = \chi_{+, \sigma}(\lambda - X)$, $H = \chi_{-, -\sigma}(\lambda + X)$, $G' = \partial_x \chi_{+, \sigma}(x + \lambda - X)|_{x=0}$, and $H' = \partial_x \chi_{-, -\sigma}(x + \lambda + X)|_{x=0}$. Equation (23) is an implicit relation between the guiding-center coordinate and the excitation energy E , yielding the dispersion relation E vs. X .

Since it is important for finding the Andreev–reflection contribution to the conductance, we also give the general expression for the amplitude ratio a/b of the wave function in the

normal region:

$$\frac{b}{a} = \frac{G' + G \left(\frac{E + \delta\lambda}{\sqrt{\Delta_0^2 - (E + \delta\lambda)^2}} c' - d' \right)}{c' H \frac{\Delta_0}{\sqrt{\Delta_0^2 - (E + \delta\lambda)^2}}}. \quad (24)$$

Further analytical progress can be made using the asymptotic expansion⁵⁴ for parabolic cylinder functions $U(\epsilon, x) \approx \frac{\Gamma(1/4 - \epsilon/2)}{2^{\epsilon/2 + 1/4} \sqrt{\pi}} \cos \left[(\epsilon/2 + 1/4)\pi \sqrt{|\epsilon|x} \right]$, being Γ the Gamma function. In our case this expansion is valid when $\epsilon_{F, n} \pm (E - \sigma g \mu_B B/2) \gg m_n \omega_c^2 (|X| + \lambda)^2$. With this, the approximated

secular equation reads

$$\cos(\varphi_{+,\sigma}) + \Omega(\varphi_{-,\sigma}) = \frac{2s}{s^2 + w^2 + 1} \frac{(E + \delta_\lambda) \sin(\varphi_{+,\sigma})}{\sqrt{\Delta_0^2 - (E + \delta_\lambda)^2}}. \quad (25)$$

Here we employed the Andreev approximation,^{8,9} i.e., assumed $E, \Delta_0, |g\mu_B B| \ll \epsilon_{F,n}, \epsilon_{F,s}$, and used the abbreviations

$$\varphi_{+,\sigma} = \pi \left[\frac{E}{\hbar\omega_c} - \frac{\sigma\eta_Z}{2} \right] + 2\sqrt{\nu} \frac{X}{l_B} - \frac{2}{\sqrt{\nu}} \left[\frac{E}{\hbar\omega_c} - \frac{\sigma\eta_Z}{2} \right] \frac{\lambda}{l_B} \quad (26a)$$

$$\varphi_{-,\sigma} = \pi \frac{\nu}{2} + \frac{2}{\sqrt{\nu}} \left[\frac{E}{\hbar\omega_c} - \frac{\sigma\eta_Z}{2} \right] \frac{X}{l_B} - 2\sqrt{\nu} \frac{\lambda}{l_B}, \quad (26b)$$

$$\Omega(\alpha) = \frac{[s^2 + w^2 - 1] \sin(\alpha) + 2w \cos(\alpha)}{s^2 + w^2 + 1}. \quad (26c)$$

The parameter $s = [\epsilon_{F,s} m_n / (\epsilon_{F,n} m_s)]^{1/2}$ measures the Fermi-velocity mismatch for the junction, and $w = [2m_n U_0^2 / (\hbar^2 \epsilon_{F,n})]^{1/2}$ quantifies interface scattering. Within the same approximation, we can write the amplitude ratio as

$$\frac{b}{a} = \mathcal{N} \frac{1 - \sin(\varphi_{+,\sigma} + \varphi_{-,\sigma}) - \left(\frac{E + \delta_\lambda}{\sqrt{\Delta_0^2 - (E + \delta_\lambda)^2}} s - w \right) \cos(\varphi_{+,\sigma} + \varphi_{-,\sigma})}{s \frac{\Delta_0}{\sqrt{\Delta_0^2 - (E + \delta_\lambda)^2}} [\sin(\varphi_{+,\sigma}) - \cos(\varphi_{-,\sigma})]}, \quad (27)$$

where

$$\mathcal{N} = \frac{\Gamma[1/4(1 + \nu - \sigma\eta_Z) + E/(2\hbar\omega_c)]}{\Gamma[1/4(1 + \nu + \sigma\eta_Z) - E/(2\hbar\omega_c)]} 2^{E/(\hbar\omega_c)}.$$

In the following, we discuss the qualitative effects of finite Zeeman splitting and screening supercurrents separately, based on our approximate analytic approach described above. While this allows us to understand certain basic features exhibited in the exact numerical results to be presented later, we caution the reader that the quantitative estimates given in the remainder of this section can be expected to apply only in limiting cases that are consistent with our approximations.

A. Finite Zeeman splitting, no screening current

Here we discuss briefly the effect of the Zeeman splitting on Andreev edge states in the absence of screening currents. We consider the case of small excitation energies, i.e. $|E - \sigma g\mu_B B| \ll \hbar\sqrt{\epsilon_{F,n}/(2m_n X^2)}$. In this situation, we find

$$E_\sigma = \Delta_0 \frac{(2n + 1)\pi \pm \arccos(\Omega_0) - 2X\sqrt{2m_n\epsilon_{F,n}}/\hbar - \frac{\pi}{2}\sigma\eta_Z}{q + \pi\Delta_0/(\hbar\omega_c)}, \quad (28)$$

where $\Omega_0 = \Omega(\pi\nu/2)$ and $q = 2s/(s^2 + w^2 + 1)$. Equation (28) is very similar to the results obtained in the absence of Zeeman interaction in Ref. 33. In particular, it shows that, at low excitation energy (those that are relevant for linear transport), the Zeeman splitting can be absorbed in a spin-dependent shift of the guiding-center coordinate X . We therefore expect the Zeeman splitting to result in the usual halving of conductance steps as a function of filling factor. As we

will see below, however, this feature manifests itself only for very transparent interfaces, while Zeeman splitting turns out to have a small effect on the conductance in realistic situations.

B. Effect of the screening current

It is immediately apparent from the general form of the secular equation that there are two important consequences of finite screening currents. First, a shift of quasiparticle energies in the superconductor by δ_λ occurs. [See Eq. (19c).] As Andreev edge states have only evanescent BdG spinor wave amplitudes in the superconductor, their formation is now possible only when the condition $\Delta_0 > |E + \delta_\lambda|$ is satisfied. Second, the spatial position corresponding to zero guiding-center coordinate of coupled electron and hole wave functions in the 2DES is shifted to $x = -\lambda$ into the superconducting region (see Fig. 1). Since the matching of BdG spinors still must be performed at the S–N interface ($x = 0$), Andreev–reflection coupling in the normal regions becomes less direct.

For a more quantitative assessment of the effect of screening currents on the Andreev–reflection conductance, we start by discussing the *ideal* interface, i.e. $w = 0$ and $s = 1$. In this case the secular equation reduces to

$$\cot(\varphi_+) = \frac{E + \delta_\lambda}{\sqrt{\Delta_0^2 - (E + \delta_\lambda)^2}}. \quad (29)$$

For zero-energy bound states ($E = 0$) and in the absence of Zeeman splitting, Eq. (29) can be transformed into the secular equation for the system *without screening current* but at *finite*

energy δ_λ and with a *renormalized filling factor*

$$\nu' = \nu \left(1 - \frac{\pi}{2} \frac{m_n}{m_s} \frac{\lambda k_{F,n}}{\nu} \right)^2. \quad (30)$$

This correspondence implies that sharp features in the linear conductance as a function of filling factor, which have their origin in the sudden appearance of new bound-state levels, are shifted to larger filling factors due to the presence of a finite screening current. In addition, the formation of zero-energy Andreev edge states will be suppressed below a critical filling factor

$$\nu_{\text{cr}} \approx \sqrt{\frac{m_n}{m_s} \frac{\epsilon_{F,n}}{\Delta_0} \lambda k_{F,n}} \quad (31)$$

because then their quasiparticle amplitudes in the superconducting region will not be evanescent. Hence, the Andreev–reflection contribution to the interface conductance vanishes for $\nu < \nu_{\text{cr}}$.

In the more typical case of a *nonideal* S–N interface, i.e., one with a nonzero interface resistance, the screening current also renormalizes the effective interface parameters s and w . Considering again zero-energy edge states in the absence of Zeeman splitting, we find new parameters

$$w_\lambda = \frac{2w \cos(2k_{F,n}\lambda) - (s^2 + w^2 - 1) \sin(2k_{F,n}\lambda)}{s^2 + w^2 + 1 - (s^2 + w^2 - 1) \cos(2k_{F,n}\lambda) - 2w \sin(2k_{F,n}\lambda)}, \quad (32a)$$

$$s_\lambda = \frac{2s}{s^2 + w^2 + 1 - (s^2 + w^2 - 1) \cos(2k_{F,n}\lambda) - 2w \sin(2k_{F,n}\lambda)}. \quad (32b)$$

III. NUMERICAL RESULTS AND DISCUSSION

We have determined the BdG spinor wave functions for zero-energy Andreev edge states numerically and calculated the Andreev–reflection contribution to the S–2DES interface conductance according to Eq. (8). Here we present results which elucidate the effects of finite Zeeman splitting and superconducting screening currents.

For the sake of clarity, we start by considering finite Zeeman splitting in the absence of screening currents and for an ideal interface. As can be seen from the dot-dashed curve in Fig. 2, a double-step structure emerges analogous to the conductance of spin-resolved quantum-Hall edge channels.⁵⁰ This feature is quickly suppressed, however, as the size of the superconducting gap increases, as well as the interface barrier becomes more opaque ($w > 0$). Using parameters that simulate a realistic NbN–InGaAs hybrid structure, Fig. 3 shows that the effect of Zeeman splitting can be expected to be rather marginal in typical samples. It results only in a suppression of the peak conductance, while the oscillatory behavior as function of filling factor remains unaffected.

Turning to the investigation of the diamagnetic screening current, we show numerical data for an ideal interface in Fig. 4. As expected from our analytical results presented in Sec. II B, we find that step features get shifted to higher filling factors as the magnetic penetration depth increases. The magnitude of the conductance is only marginally affected. Interestingly, an improvement of step quality is clearly apparent for increasing penetration depth. As in the case without screening current, step-like features disappear and are replaced by an oscillatory conductance as soon as the interface is nonideal. This can be seen in Fig. 5, where the effect of interface scattering in the presence of screening currents is

illustrated. While some of the sharp features of the step structure remain, the Andreev–reflection contribution to the conductance is much suppressed by an interface barrier. It does reach a value comparable to the ideal case ($w = 0, s = 1$) only at specific values of filling factor.

Finally, the behavior of the conductance in a realistic S–2DES hybrid structure with screening supercurrents present is

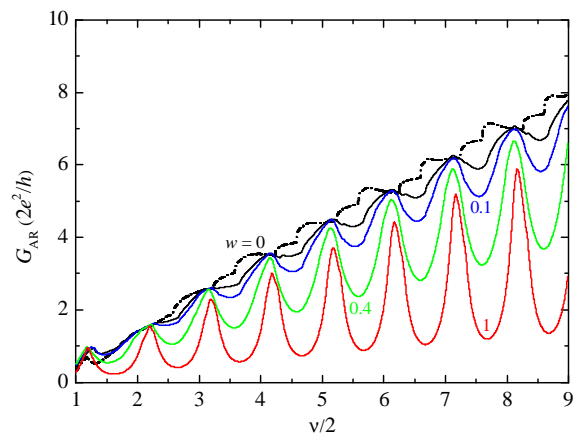


FIG. 2: Effect of Zeeman splitting on the Andreev–reflection contribution to the S–N interface conductance G_{AR} . A double-step structure is clearly visible for the dot-dashed curve which has been calculated for an ideal interface ($s = 1, w = 0$) and $g = -20$, $\Delta_0 = 0.3$ meV, $\epsilon_{F,s} = \epsilon_{F,n} = 10$ meV, and $m_s = m_n = 0.035m_e$. This feature turns out to be obscured at larger values of the superconducting gap ($\Delta_0 = 3$ meV for all solid curves), in particular when an interface barrier is present (nonzero values of w as indicated for each curve).

shown in Fig. 6. Vanishing of the conductance below a critical filling factor arises from the disappearance of zero-energy bound states due to the Doppler shift of quasiparticles in the superconductor which reduces the excitation gap to zero.⁴⁵ As the quasiparticles become propagating in the S-region, Andreev reflection at the interface is suppressed. This has important consequences for experimental investigation of Andreev edge states. The results shown in Fig. 6 indicate that, for a S electrode made from a NbN film for which $\lambda \sim 400$ nm has been reported in the literature,⁵⁵ effects due to Andreev reflection at the interface may be visible only at rather large values of the filling factor.

IV. CONCLUSIONS

We have investigated the interplay between Andreev reflection and cyclotron motion at S–N interfaces. The effects of Zeeman splitting in the normal region and diamagnetic screening currents in the superconductor have been taken into account. In the ideal case, Zeeman splitting results in a doubling of step features in the Andreev–reflection contribution to the interface conductance, and screening currents lead to a shift of such features to larger filling factors. However, in realistic S–2DES hybrid structures, the Zeeman splitting turns out to merely suppress peak conductance. Screening currents turn out to be important because the Doppler shift of quasiparticles in the S–region will suppress their energy gap to zero below a critical filling factor, making Andreev reflection disappear altogether. Above this critical value, the typical oscillatory structure of the Andreev reflection contribution to the interface conductance is displayed.

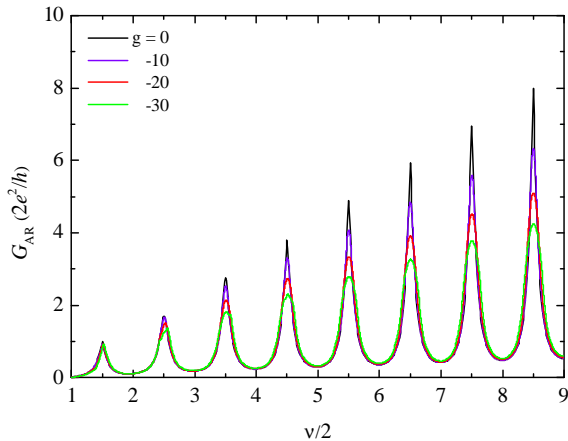


FIG. 3: Effect of Zeeman splitting for a realistic S–2DEG junction realized, e.g., by a typical NbN/InGaAs hybrid system: $\epsilon_{F,s} = 7$ eV, $\epsilon_{F,n} = 10$ meV, $m_s = m_e$, $m_n = 0.035m_e$, $\Delta_0 = 3$ meV, $w = 0$, and for various values of the gyromagnetic factor g as indicated.

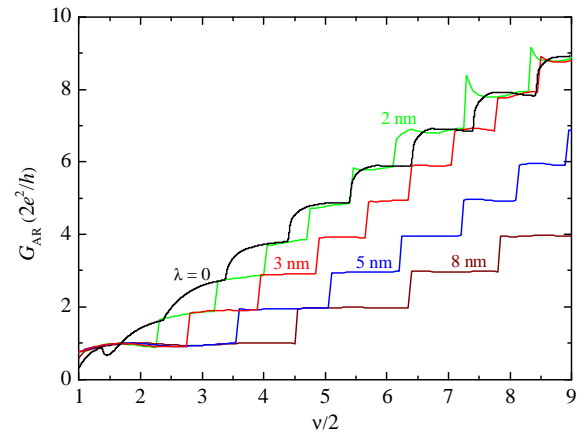


FIG. 4: Diamagnetic screening currents lead to a shift of conductance steps. Data shown are calculated for an ideal interface ($s = 1$, $w = 0$), $g = 0$, $\Delta_0 = 0.3$ meV, $\epsilon_{F,s} = \epsilon_{F,n} = 10$ meV, and $m_s = m_n = 0.035m_e$ for various values of the magnetic penetration depth λ .

Acknowledgments

The authors wish to thank Rosario Fazio for fruitful discussions and for critical reading of the manuscript. UZ gratefully acknowledges the hospitality of Scuola Normale Superiore in Pisa during a visit when work on this project was completed. This work was partially supported by FIRB “Nanotechnologies and Nanodevices for Information Society”, contract RBNE01FSWY.

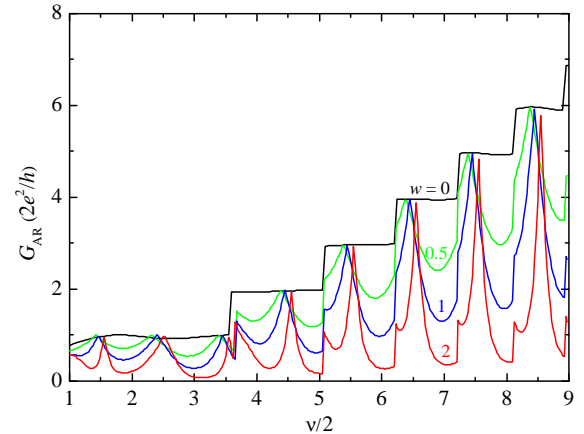


FIG. 5: Andreev–reflection transport at high magnetic fields through a nonideal S–N interface with diamagnetic screening current present. Results shown are for $\lambda = 5$ nm and various values of w as indicated, with all other parameters as given in Fig. 4.

¹ E. Akkermans, G. Montambaux, J.-L. Pichard, and J. Zinn-Justin (Eds.), *Mesoscopic Quantum Physics* (Elsevier Science, Amster-

dam, 1995).

- ² L. L. Sohn, L. P. Kouwenhoven, and G. Schön (Eds.), *Mesoscopic Electron Transport*, vol. 345 of *NATO ASI Series E* (Kluwer Academic, Dordrecht, 1997).
- ³ Y. Imry, *Introduction to Mesoscopic Physics*, 2nd Ed. (Oxford University Press, NY, 2002).
- ⁴ F. W. J. Hekking, G. Schön, and D. V. Averin (Eds.), *Mesoscopic Superconductivity* (Elsevier Science, Amsterdam, 1994), Special Issue of *Physica B* **203**.
- ⁵ C. W. J. Beenakker, in Ref. 1, pp. 291–324.
- ⁶ C. J. Lambert and R. Raimondi, *J. Phys.: Condens. Matter* **10**, 901 (1998).
- ⁷ B. J. van Wees and H. Takayanagi, in Ref. 2, pp. 469–501.
- ⁸ A. F. Andreev, *Zh. Eksp. Teor. Fiz.* **46**, 1823 (1964) [*Sov. Phys. JETP* **19**, 1228 (1964)].
- ⁹ A. F. Andreev, *Zh. Eksp. Teor. Fiz.* **49**, 655 (1965) [*Sov. Phys. JETP* **22**, 455 (1966)].
- ¹⁰ I. O. Kulik, *Zh. Eksp. Teor. Fiz.* **57**, 1745 (1969) [*Sov. Phys. JETP* **30**, 944 (1970)].
- ¹¹ A. D. Zaikin and G. F. Zharkov, *Zh. Eksp. Teor. Fiz.* **78**, 721 (1978) [*Sov. Phys. JETP* **51**, 364 (1980)].
- ¹² M. J. M. de Jong and C. W. J. Beenakker, *Phys. Rev. Lett.* **74**, 1657 (1995).
- ¹³ R. J. Soulen, J. M. Byers, M. S. Osofsky, B. Nadgorny, T. Ambrose, S. F. Cheng, P. R. Broussard, C. T. Tanaka, J. Nowak, J. S. Moodera, A. Barry, and J. M. D. Coey, *Science* **282**, 85 (1998).
- ¹⁴ S. K. Upadhyay, A. Palanisami, R. N. Louie, and R. A. Buhrman, *Phys. Rev. Lett.* **81**, 3247 (1998).
- ¹⁵ Y. Aharonov and D. Bohm, *Phys. Rev.* **115**, 485 (1959).
- ¹⁶ V. P. Galaiko, *Zh. Eksp. Teor. Fiz.* **57**, 941 (1969) [*Sov. Phys. JETP* **30**, 514 (1970)].
- ¹⁷ V. P. Galaiko and E. V. Bezuglyi, *Zh. Eksp. Teor. Fiz.* **60**, 1471 (1972) [*Sov. Phys. JETP* **33**, 796 (1971)].
- ¹⁸ G. A. Gogadze and I. O. Kulik, *Zh. Eksp. Teor. Fiz.* **60**, 1819 (1971) [*Sov. Phys. JETP* **33**, 984 (1971)].
- ¹⁹ T. N. Antsygina, E. N. Bratus', and A. V. Svidzinskii, *Fiz. Nizk. Temp.* **1**, 49 (1975) [*Sov. J. Low Temp. Phys.* **1**, 29 (1975)].
- ²⁰ A. D. Zaikin, *Solid St. Commun.* **41**, 533 (1982).
- ²¹ W. Belzig, C. Bruder, and A. L. Fauchère, *Phys. Rev. B* **58**, 14531 (1998).
- ²² U. Ledermann, A. L. Fauchère, and G. Blatter, *Phys. Rev. B* **59**, R9027 (1999).

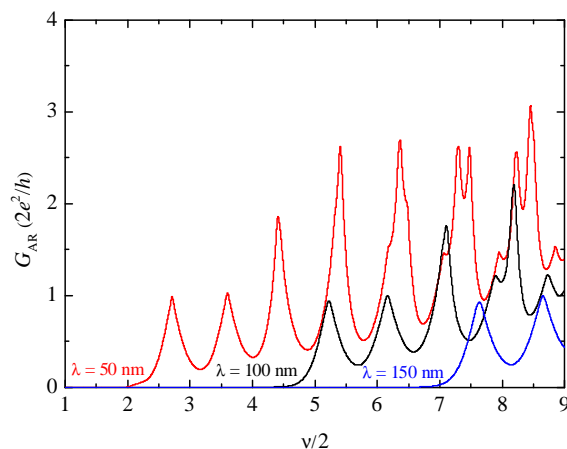


FIG. 6: Effect of the diamagnetic screening current at a realistic S–2DEG interface such as in a NbN/InGaAs hybrid system, but for $g = 0$. Sample parameters are the same as for Fig. 3.

- ²³ For a recent review of quasiclassical methods in mesoscopic superconductivity, see, e.g., W. Belzig, F. K. Wilhelm, G. Schön, C. Bruder, and A. D. Zaikin, *Superlatt. Microstruct.* **25**, 1251 (1999).
- ²⁴ L. D. Landau, *Z. Phys.* **64**, 629 (1930).
- ²⁵ R. E. Prange and S. M. Girvin (eds.), *The Quantum Hall Effect*, 2nd Ed. (Springer, New York, 1990).
- ²⁶ T. Chakraborty and P. Pietiläinen, *The Quantum Hall Effects*, 2nd Ed. (Springer, Berlin, 1995).
- ²⁷ H. Takayanagi and T. Akazaki, *Physica B* **249–251**, 462 (1998).
- ²⁸ T. D. Moore and D. A. Williams, *Phys. Rev. B* **59**, 7308 (1999).
- ²⁹ D. Uhlir, S. G. Lachenmann, T. Schäpers, A. I. Braginski, H. Lüth, J. Appenzeller, A. A. Golubov, and A. V. Ustinov, *Phys. Rev. B* **61**, 12463 (2000).
- ³⁰ I. E. Batov, T. Schäpers, A. A. Golubov, and A. V. Ustinov, *J. Appl. Phys.* **96**, 3366 (2004).
- ³¹ J. Eroms, D. Weiss, J. De Boeck, and G. Borghs, cond-mat/0404323 (unpublished).
- ³² Y. Takagaki, *Phys. Rev. B* **57**, 4009 (1998).
- ³³ H. Hoppe, U. Zülicke, and G. Schön, *Phys. Rev. Lett.* **84**, 1804 (2000).
- ³⁴ Y. Asano, *Phys. Rev. B* **61**, 1732 (2000).
- ³⁵ Y. Asano and T. Kato, *J. Phys. Soc. Jpn.* **69**, 1125 (2000).
- ³⁶ Y. Asano and T. Yuito, *Phys. Rev. B* **62**, 7477 (2000).
- ³⁷ U. Zülicke, H. Hoppe, and G. Schön, *Physica B* **298**, 453 (2001).
- ³⁸ N. M. Chtchelkachev, *JETP Lett.* **73**, 9497 (2001).
- ³⁹ G. Tkachov and V. I. Fal'ko, *Phys. Rev. B* **69**, 092503 (2004).
- ⁴⁰ Early theoretical work considered tunnel contacts between superconductors and quantum-Hall systems. See M. Ma and A. Yu. Zyuzin, *Europhys. Lett.* **21**, 941 (1993); M. P. A. Fisher, *Phys. Rev. B* **49**, 14550 (1994); A. Yu. Zyuzin, *ibid.* **50**, 323 (1994); Y. Ishikawa and H. Fukuyama, *J. Phys. Soc. Jpn.* **68**, 954 (1999).
- ⁴¹ A recent study of the interplay between Zeeman splitting and screening currents at a S–2DES junction subject to an *inplane* magnetic field (i.e., in the absence of cyclotron motion) is reported in G. Tkachov and K. Richter, *Phys. Rev. B* **71**, 094517 (2005).
- ⁴² A. G. Aronov and A. S. Ioselevich, *Zh. Eksp. Teor. Fiz.* **74**, 580 (1978) [*Sov. Phys. JETP* **47**, 305 (1978)].
- ⁴³ Note that cyclotron orbits of electrons and holes have the same chirality. This is due to the fact that the Andreev–reflection process reverses the sign not only of group velocity and charge but also of the mass of an incoming particle. Early experiments used this property to observe Andreev reflection directly with the help of magnetic focusing. See S. I. Bozhko, V. S. Tsoi, and S. E. Yokovlev, *Pis'ma Zh. Eksp. Teor. Fiz.* **36**, 123 (1982) [*JETP Lett.* **36**, 153 (1983)]; P. A. M. Benistant, H. van Kempen, and P. Wyder, *Phys. Rev. Lett.* **51**, 817 (1983).
- ⁴⁴ A. H. MacDonald, in Ref. 1, pp. 659–720.
- ⁴⁵ P. G. de Gennes, *Superconductivity of Metals and Alloys* (Addison-Wesley, Reading, MA, 1989).
- ⁴⁶ G. E. Blonder, M. Tinkham, and T. M. Klapwijk, *Phys. Rev. B* **25**, 4515 (1982).
- ⁴⁷ B. I. Halperin, *Phys. Rev. B* **25**, 2185 (1982).
- ⁴⁸ A. H. MacDonald and P. Středa, *ibid.* **29**, 1616 (1984).
- ⁴⁹ M. Büttiker, *Phys. Rev. B* **38**, 9375 (1988).
- ⁵⁰ R. J. Haug, *Semicond. Sci. Technol.* **8**, 131 (1993).
- ⁵¹ See textbooks on quantum mechanics, e.g., C. Cohen–Tannoudji, B. Diu, and F. Laloë, *Quantum Mechanics*, vol. II (Wiley, New York, 1977). The original works are H. Hellmann, *Einführung in die Quantenchemie* (Deuticke, Leipzig, 1937), Sec. 54; R. P. Feynman, *Phys. Rev.* **56**, 340 (1939).
- ⁵² N. A. Mortensen, K. Flensberg, and A.-P. Jauho, *Phys. Rev. B* **59**, 10176 (1999).
- ⁵³ J. B. Ketterson and S. N. Song, *Superconductivity* (Cambridge University Press, Cambridge, UK, 1999).

⁵⁴ M. Abramowitz and I. A. Stegun, *Handbook of Mathematical Functions* (Dover Publications, New York, 1972).

⁵⁵ M. S. Pambianchi, S. M. Anlage, E. S. Hellmann, E. H. Hartford,

M. Bruns, and S. Y. Lee, *Appl. Phys. Lett.* **64**, 244 (1994).